Piezoelectric field, exciton lifetime, and cathodoluminescence intensity at threading dislocations in GaN{0001}

Vladimir M. Kaganer, Karl K. Sabelfeld, and Oliver Brandt

Citation: Appl. Phys. Lett. **112**, 122101 (2018); doi: 10.1063/1.5022170
View online: https://doi.org/10.1063/1.5022170
View Table of Contents: http://aip.scitation.org/toc/apl/112/12
Published by the American Institute of Physics

Piezoelectric field, exciton lifetime, and cathodoluminescence intensity at threading dislocations in GaN{0001}

Vladimir M. Kaganer,[1] Karl K. Sabelfeld,[2] and Oliver Brandt[1]
[1]*Paul-Drude-Institut für Festkörperelektronik, Hausvogteiplatz 5–7, 10117 Berlin, Germany*
[2]*Institute of Computational Mathematics and Mathematical Geophysics, Russian Academy of Sciences, Lavrentiev Prosp. 6, 630090 Novosibirsk, Russia*

(Received 11 January 2018; accepted 5 March 2018; published online 19 March 2018)

The strain field of a dislocation emerging at a free surface is partially relaxed to ensure stress free boundary conditions. We show that this relaxation strain at the outcrop of edge threading dislocations in GaN{0001} gives rise to a piezoelectric volume charge. The electric field produced by this charge distribution is strong enough to dissociate free excitons at distances over 100 nm from the dislocation line. We evaluate the impact of this effect on cathodoluminescence images of dislocations. *Published by AIP Publishing*. https://doi.org/10.1063/1.5022170

Cathodoluminescence (CL) maps of GaN{0001} surfaces reveal threading dislocations as dark spots, directly demonstrating that they act as centers of nonradiative recombination of excitons.[1–4] The nonradiative recombination process is commonly presumed to take place at the dislocation core. The size of the dark spots, typically some 100 nm in diameter, is understood to be a result of exciton diffusion, and intensity profiles across the dislocation have been used frequently to extract quantitative information on the exciton diffusion length.[1–11]

Wurtzite GaN is a pyroelectric (and thus piezoelectric) crystal. Uniform strain produces a piezoelectric polarization, and strain variations generate a piezoelectric field that may dissociate excitons. In bulk GaN, neither *a*-type edge nor *c*-type screw dislocations with the line direction along $\langle 0001 \rangle$ cause piezoelectric fields,[12,13] in contrast to dislocations with other line directions. When these dislocations reach a surface, a polarization charge is created due to the discontinuity of the piezoelectric polarization as well as the spontaneous polarization. In a previous work, this charge was presumed to be screened by free charges in surface states, and it was concluded that the piezoelectric fields of threading dislocations have a minimal effect on the electric and optical properties of GaN{0001}.[13]

These considerations were based on the strain field of a straight dislocation in bulk GaN, which does not vary along the *c* axis. However, the strain field of the dislocation changes in the vicinity of the surface to produce a stress-free boundary.[14,15] The resulting three-dimensional electric field at the dislocation outcrop in GaN{0001} was calculated numerically by a finite element approach[16] as an illustration of the computational method, but the consequences of this field were not considered.

In the present work, we calculate the distribution of the piezoelectric field that arises due to elastic strain relaxation at the surface around the outcrops of threading dislocations in GaN{0001}. This field drastically reduces the exciton lifetime close to the dislocation outcrop. We calculate the CL image of the dislocation in the absence of exciton diffusion, with exciton dissociation being the only reason for a variation of the CL signal near the dislocation. The widths of the CL intensity profiles thus obtained can approach the widths of the profiles observed experimentally.

A rigorous calculation of the piezoelectric field requires us to take into account both the direct (polarization caused by strain) and the converse (stress caused by electric field) piezoelectric effects, necessitating a selfconsistent solution of the coupled equations of elasticity and electrostatics.[17–21] The relative contributions of the two effects and the need for the rigorous solution are examined in the following by the order of magnitude estimates. In the next two paragraphs, the orientational dependencies and the indices of the respective tensors are omitted and the sign $\sim$ means "on the order of."

The direct effect results in a polarization $P \sim e\varepsilon$, where e and ε are the characteristic magnitudes of the piezoelectric constants and the strain, respectively. The converse effect produces a stress $\sigma \sim eE$ with the electric field E and the same piezoelectric constants e as for the direct effect. This stress is added to the stress $\sigma \sim C\varepsilon$ caused by elastic strain (here, C is the characteristic magnitude of the elastic moduli). As a first approximation, the electric field can be taken to be equal to that induced by the direct effect, $E \sim P/\kappa_0\kappa$, where κ_0 is the vacuum permittivity and $\kappa = 9.5$ is the relative permittivity of GaN. Substituting this field results in a stress of $\sigma \sim (1 + K^2)C\varepsilon$, where $K^2 = e^2/\kappa_0\kappa C$ is the electromechanical coupling constant (in a precise definition, this constant is expressed through the components of the involved tensors and depends on directions in the crystal[19]). This dimensionless quantity controls the ratio of the converse to direct piezoelectric effects. Taking for the estimate $e \sim e_0/a^2 \sim 1\,\mathrm{C\ m^{-2}}$ with the elementary charge e_0 and the lattice constant a, and $C = 200\,\mathrm{GPa}$, we arrive at $K^2 = 0.06$. This estimate agrees with the impact of the converse piezoelectric effect in planar heteroepitaxial structures.[21]

In addition to the piezoelectric effect, the spatially varying strain field of a dislocation gives rise to a polarization due to the flexoelectric effect. This effect takes place in all dielectric materials and induces a polarization $P \sim f\,\mathrm{grad}\,\varepsilon$ (see Refs. 22–24 and references therein). With the characteristic magnitude of the flexoelectric constants $f \sim e_0/a$ and the dislocation strain $\varepsilon \sim b/2\pi r_\perp$ (where b is the Burgers vector and $r_\perp$ is the distance from the dislocation line), the ratio of the flexoelectric and piezoelectric effects is $\sim a/r_\perp$. Hence, when

distances from the dislocation are large in comparison with the atomic distances, the flexoelectric effect can be neglected.

Given the fact that the converse piezoelectric and the flexoelectric effects result in corrections of only a few percent, much less than the uncertainty introduced by the low accuracy with which the piezoelectric constants are known, we do not include them in the following calculations. In this case, the piezoelectric polarization $\boldsymbol{P}$ caused by strain in a crystal with the wurtzite structure has the components

$$P_x = 2e_{15}\varepsilon_{xz}, \quad P_y = 2e_{15}\varepsilon_{yz},$$
$$P_z = e_{31}(\varepsilon_{xx} + \varepsilon_{yy}) + e_{33}\varepsilon_{zz}, \tag{1}$$

where e_{13}, e_{33}, and e_{15} are the piezoelectric constants of the wurtzite structure and ε_{ij} are the components of the strain tensor. The z axis is directed along the [0001] direction. Using analytical expressions for the displacement field of an edge dislocation normal to the surface[14,15] and calculating the corresponding components of the strain tensor, the components of the polarization vector, and the polarization charge density $\varrho(\boldsymbol{r}) = -\mathrm{div}\,\boldsymbol{P}$, we obtain

$$\varrho(\boldsymbol{r}) = y\left(\frac{f_1}{r^3} + \frac{f_2 z^2}{r^5}\right), \tag{2}$$

where $r = (x^2 + y^2 + z^2)^{1/2}$ and

$$f_1 = \frac{b}{\pi}\frac{\nu}{1-\nu}[\nu e_{33} - (1-\nu)e_{31}], \tag{3}$$

$$f_2 = \frac{3b}{2\pi}\frac{\nu}{1-\nu}(e_{31} + 2e_{15} - e_{33}), \tag{4}$$

with the Poisson ratio ν. We restrict our calculations to the elastically isotropic case. The expressions for the displacement field of an edge dislocation far from the surface, written for an isotropic medium, remain valid for an edge dislocation in the elastically anisotropic hexagonal crystal with the dislocation line along the c axis, if the Poisson ratio is taken as $\nu = C_{12}/(C_{11} + C_{12})$, where C_{ij} are the elastic moduli.[25] With the elastic moduli of GaN,[26] we obtain $\nu = 0.27$. We also use this value for the relaxation displacement field.

The piezoelectric constants of GaN obtained in different experiments and *ab initio* calculations are reviewed in Ref. 27. The values of e_{31} scatter from –0.22 to –0.55 C m^{-2}, while e_{33} ranges from 0.43 to 1.12 C m^{-2}. With regard to e_{15}, the reported values vary from –0.40 to 0.33 C m^{-2}, i.e., not even its sign is clear. For the numerical examples below, we take the calculated values[28] $e_{31} = -0.527$ C m^{-2} and $e_{33} = 0.895$ C m^{-2} and assume $e_{15} = e_{31}$. The latter equality is a common simplification justified by analogy with the cubic phase of GaN, for which both constants can be expressed through its only piezoelectric coefficient e_{14}. This analogy is believed to be an oversimplification, however.[27] We find a rather strong dependence of the cathodoluminescence intensity in our calculations on the value of e_{15} as discussed at the end of this paper. With the values of the piezoelectric constants chosen above and with the Burgers vector of an a-type edge dislocation $b = 0.319$ nm, we obtain the values $f_1 = 0.235 \times 10^{-10}$ C m^{-1} and $f_2 = -1.39 \times 10^{-10}$ C m^{-1}.

We have performed the same calculation for the charge density for a c-type screw dislocation. The strain relaxation at the free surface gives rise to a non-zero piezoelectric polarization $\boldsymbol{P}$, but the charge density $\varrho(\boldsymbol{r}) = -\mathrm{div}\,\boldsymbol{P}$ is equal to zero. Hence, screw threading dislocations do not generate a piezoelectric field. Since the equations of both elasticity and electrostatics are linear, mixed ($a + c$-type) dislocations produce the same piezoelectric field as a-type edge dislocations.

To obtain the piezoelectric field associated with the charge density (2), we consider first the case of undoped GaN so that free charges in the bulk are absent and the electric potential $V(\boldsymbol{r})$ is the solution of the Poisson equation

$$\nabla^2 V = -\frac{\varrho}{\kappa_0 \kappa}. \tag{5}$$

We assume that the surface charges are screened by free charges so that the boundary condition for Eq. (5) reads $V|_{z=0} = 0$.

The solution of Eq. (5) for a point charge with the equipotential boundary condition $V|_{z=0} = 0$ is the Coulomb potential $1/4\pi\kappa_0\kappa r$ plus that of the image (of the opposite sign) with respect to the surface $z = 0$. Integrating the point charge solution with the charge distribution (2), we arrive at the potential

$$V(x,y,z) = V_0 \frac{yz}{r_\perp^2}\left[\left(1 - \frac{z}{r}\right) + \frac{f_2}{6f_1}\left(1 - \frac{z^3}{r^3}\right)\right], \tag{6}$$

where $V_0 = f_1/2\kappa_0\kappa$ and $r_\perp = (x^2 + y^2)^{1/2}$. We do not present the details of the derivation since the result can be directly verified by differentiating expression (6) and checking that Eq. (5) is satisfied with the charge density (2).

With the numerical values of the material parameters of GaN given above, we find $V_0 = 0.139$ V and $f_2/6f_1 = -0.988$. Taking $f_2/6f_1 = -1$, Eq. (6) simplies to

$$V(x,y,z) \approx -V_0 \frac{yz^2}{r^3}. \tag{7}$$

The piezoelectric field is given by $\boldsymbol{E} = -\mathrm{grad}\,V$. Since the exciton lifetime depends on the magnitude of the electric field $E = |\boldsymbol{E}|$ rather than its direction, we visualize the field distribution in Fig. 1 by plotting an iso-field surface. The shape of this surface does not depend on E and scales with its value since $E \propto r^{-1}$. The three-dimensional surface of the constant electric field at $E = 10$ kV/cm shown in the figure extends to distances of about 70 nm from the dislocation line and to a depth up to 140 nm from the surface.

The dissociation rate $1/\tau_E$ of the free exciton in the electric field E is calculated analogously to the ionization probability (per unit time) of the hydrogen atom.[29–31] It can be expressed as

$$\frac{1}{\tau_E} = \omega \frac{4E_0}{E}\exp\left(-\frac{2E_0}{3E}\right), \tag{8}$$

where the frequency ω and the electric field E_0 are given in terms of the exciton binding energy $\mathcal{E}$ as $\omega = \mathcal{E}/\hbar$ and $E_0 = 2\mathcal{E}/e_0 a_B$. Here, $\hbar$ is the reduced Planck constant, $a_B = 4\pi\kappa_0\kappa\hbar^2/e_0^2\mu$ is the Bohr radius, and μ is the reduced mass of the exciton (equal to 0.18 electron masses for the free A exciton in GaN). The exciton binding energy is $\mathcal{E} = \hbar^2/2\mu a_B^2$. We

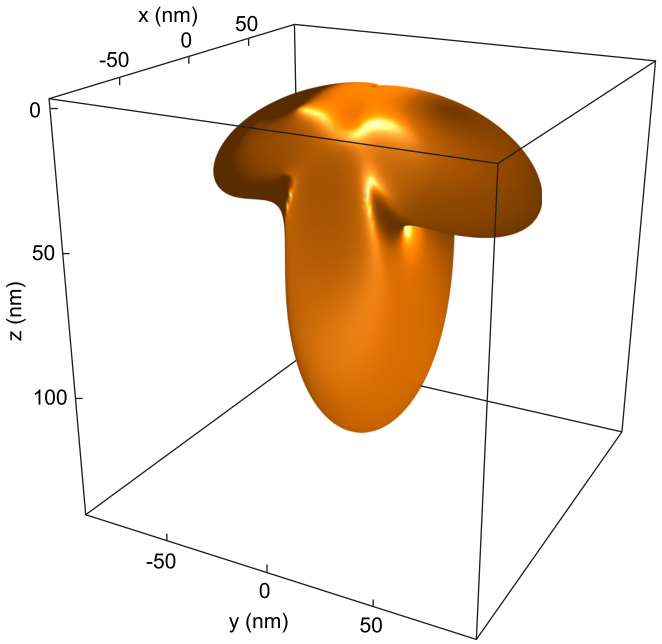

FIG. 1. Electric field distribution $E = |\boldsymbol{E}|$ around the outcrop of an edge threading dislocation. The figure shows an iso-field surface at $E = 10\,\mathrm{kV/cm}$. The xy plane at $z = 0$ corresponds to the GaN{0001} surface.

thus obtain $e_0\mathcal{E} = 27\,\mathrm{meV}$, $\omega = 4.1 \times 10^{13}\,\mathrm{s}^{-1}$, and $E_0 = 193\,\mathrm{kV/cm}$. As an example, for the electric field $E = 10\,\mathrm{kV/cm}$ shown in Fig. 1, the characteristic dissociation time of the exciton is $\tau_E = 0.12\,\mathrm{ns}$, i.e., notably smaller than the typical effective exciton lifetime in epitaxial GaN layers. Since electrons and holes are rapidly separated by the piezoelectric field and one carrier type will be driven toward the dislocation, this process constitutes an effectively nonradiative decay channel by dissociating excitons already at distances of about 100 nm from the dislocation line. Equation (8) is derived for small electric fields such that $E \ll E_0$. This condition does not restrict our considerations since, when E becomes comparable with E_0, the lifetime τ_E is so small that the dissociation process can be considered as being instantaneous.

To demonstrate the effect of the electric field displayed in Fig. 1 on exciton recombination in the absence of exciton diffusion, we calculate a CL image around an edge threading dislocation intersecting the GaN{0001} surface. Electron-hole pairs are generated by the primary electron beam with an acceleration voltage of 3 kV. The spatial distribution $Q(\boldsymbol{r})$ of these pairs, which is assumed to correspond to the distribution of free A excitons with wavevector $\boldsymbol{K} = 0$, is obtained with the help of the free software CASINO.[32] The effective exciton lifetime including exciton dissociation by the piezoelectric field is calculated according to

$$\frac{1}{\tau_{\mathrm{eff}}(\boldsymbol{r})} = \frac{1}{\tau_r} + \frac{1}{\tau_{nr}} + \frac{1}{\tau_E(\boldsymbol{r})}, \tag{9}$$

where τ_r and τ_{nr} are the radiative and nonradiative lifetimes far from the dislocation, respectively, and $\tau_E(\boldsymbol{r})$ is given by Eq. (8). We take $\tau_r = 200\,\mathrm{ns}$ and $\tau_{nr} = 1\,\mathrm{ns}$, neglecting any dependence of these values on the electric field. The CL intensity is then calculated as a convolution

$$I_{\mathrm{CL}}(\boldsymbol{r}) = \tau_r^{-1} \int \tau_{\mathrm{eff}}(\boldsymbol{r}')Q(\boldsymbol{r} - \boldsymbol{r}')d\boldsymbol{r}'. \tag{10}$$

The calculated CL map and the intensity profiles along (x direction) and perpendicular to (y direction) the Burgers vector of the dislocation are presented in Figs. 2(a) and 2(b). Longer nonradiative lifetimes would produce profiles with a somewhat larger width. The dependence of the width on the lifetime is, however, rather weak since $\tau_E(\boldsymbol{r})$ sharply varies with the distance from the dislocation.

The inset in Fig. 2(a) shows, on the same scale as the CL map, the spatial distribution $Q(\boldsymbol{r})$ of the electron-hole pairs generated by the electron beam. The figure shows the projection of the three-dimensional distribution on the xz plane. The majority of electron-hole pairs is generated in a region with a lateral width of only a few nm so that the spatial extension of the dislocation image in Fig. 2 is entirely determined by the piezoelectric field. This width of about 100 nm is on the same order as the one observed in experimentally recorded CL images.[1–11] The image is notably extended in the y direction (the direction of the extra half-plane of the dislocation). This asymmetry is

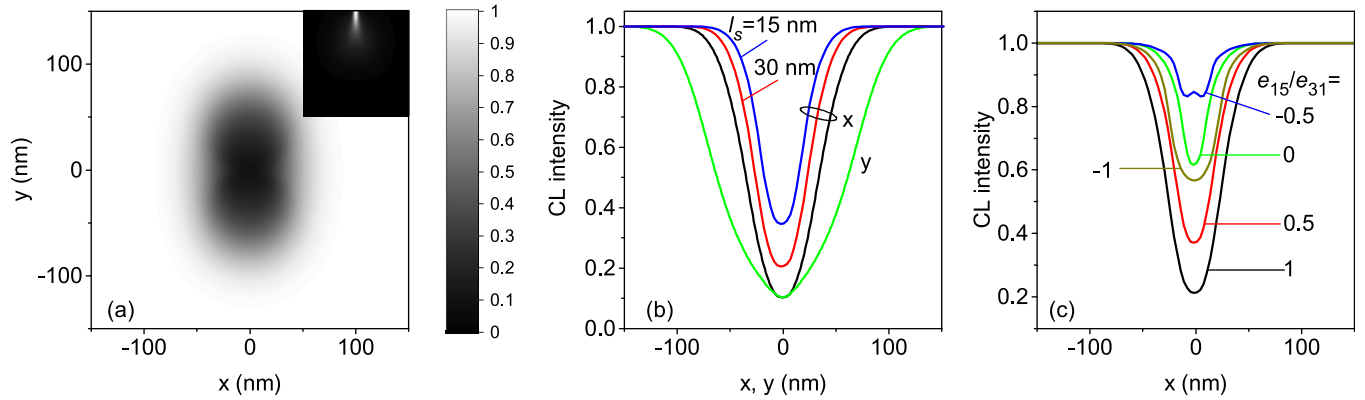

FIG. 2. Calculated CL intensity map around an edge threading dislocation in GaN{0001} in the absence of exciton diffusion. The acceleration voltage of the electron beam generating electron-hole pairs is 3 kV. (a) Two-dimensional CL intensity distribution and (b) scans parallel (x direction) and perpendicular (y direction) to the Burgers vector of the dislocation. The inset in (a) shows the distribution of the electron-hole pairs generated by the electron beam on the same scale as the CL intensity map. The map in (a) is calculated for an unscreened piezoelectric charge distribution. The profile along x in (b) is compared with the ones calculated for the piezoelectric charges screened by free carriers with densities 6×10^{16} and $1.5 \times 10^{16}\,\mathrm{cm}^{-3}$, resulting in room temperature Debye lengths of 15 and 30 nm, respectively. (c) Calculated CL intensity profiles for different ratios e_{15}/e_{31} in the direction parallel to the Burgers vector for the Debye screening length of 30 nm.

expected to be smoothed out, at least partially, by diffusion of excitons.

Unintentionally doped GaN layers usually exhibit an *n*-type background doping due to the incorporation of the shallow donors O and Si. These free electrons will screen the fields induced by the piezoelectric polarization charges. We follow the Debye-Hückel approximation for piezoelectric semiconductors[33–35] and include in the Poisson equation (5) an additional free charge distribution $\tilde{\varrho}(\boldsymbol{r}) = ne_0 \exp(e_0V/k_BT)$, where n is the electron density, k_B is the Boltzmann constant, and T is the temperature. Then, after expansion over $e_0V \ll k_BT$ up to the linear term, Eq. (5) is replaced with

$$\nabla^2 V - k_s^2 V = -\frac{\varrho}{\kappa_0\kappa}, \tag{11}$$

where the inverse screening length k_s is given by $k_s = (e_0^2 n/\kappa_0\kappa k_B T)^{1/2}$. For an electron density of $n = 6\times 10^{16}\,\mathrm{cm}^{-3}$ at room temperature, the Debye screening length is $l_s = 1/k_s = 15\,\mathrm{nm}$.

The solution of Eq. (11) for a point charge, which ensures the equipotential surface $V|_{z=0} = 0$, is the screened Coulomb potential $\exp(-k_s r)/4\pi\kappa_0\kappa r$ plus that of its image (of the opposite sign) with respect to the surface $z = 0$. To calculate the convolution integral of the charge distribution (2) with the point charge solution, we represent the charge distribution (2) as a Fourier integral

$$\varrho(x,y,z) = \frac{y}{r_\perp}\int_0^\infty q\,dq\,J_1(qr_\perp)\left(f_1 + \frac{f_2}{3}qz\right)e^{-qz}, \tag{12}$$

and arrive at the potential

$$V = \frac{2V_0}{k_s^2}\frac{y}{r_\perp}\int_0^\infty q\,dq J_1(qr_\perp) \times\left[\left(1-\frac{2f_2}{3f_1}\frac{q^2}{k_s^2}\right)\left(e^{-qz} - e^{-\sqrt{k_s^2+q^2}z}\right) + \frac{f_2}{3f_1}qze^{-qz}\right]. \tag{13}$$

This solution can be directly verified by differentiating the potential (13) and checking that the screened Poisson equation (11) is satisfied with the charge distribution (12). In the limit $k_s \to 0$, the potential (13) reduces to Eq. (6).

Figure 2(b) shows that the screening of the piezoelectric field reduces both the width of the dislocation image and its contrast. The region of the electric field, large enough to dissociate excitons, decreases due to screening both laterally and in depth. The reduction in the lateral direction results in a narrowing of the dislocation image. Its reduction in the depth decreases the probability of nonradiative recombination for excitons created at larger depths and hence reduces the contrast of the dislocation image. The effect of the piezoelectric field reduces with increasing acceleration voltage of the electron beam since the piezoelectric field is restricted in depth while the excitons are produced deeper in the crystal. Then, the nonradiative recombination at the dislocation core, along the whole dislocation line, becomes the primary mechanism of the dislocation contrast.

We now return to the choice of the piezoelectric constant e_{15}. Since the e_{15} values reported in the literature[27] range from approximately e_{31} to $-e_{31}$, we calculate the CL intensity profiles for e_{15} varying in this range. Figure 2(c) shows the profiles along the Burgers vector for a Debye screening length of $l_s = 30\,\mathrm{nm}$. The contrast of the CL intensity profiles is seen to depend sensitively on the choice of e_{15}. Our initial assumption $e_{15} = e_{31}$ gives rise to the strongest contrast, which is larger than that usually observed experimentally.[1–11] Hence, the magnitude of e_{15} seems to be smaller than e_{31}, or its sign is even positive.

To summarize and conclude, the strain field of an edge threading dislocation relaxes at the surface to achieve a stress-free boundary. The resulting strain field causes an inhomogeneous distribution of piezoelectric polarization charges which, in turn, induces a volume electric field around the dislocation outcrop. Excitons dissociate in this electric field, thus reducing the exciton lifetime. Even in the absence of exciton diffusion, dislocations in undoped GaN give rise to dark spots in CL maps with diameters up to 100 nm. The Debye-Hückel screening of the piezoelectric field by free carriers reduces the image diameter. However, its width remains significant when compared to experimentally recorded CL intensity profiles of dislocations. Thus, the exciton diffusion length may be notably smaller than it is usually inferred from CL images of dislocations. We will study the effect of exciton diffusion in the presence of the piezofield at the dislocation outcrop in a forthcoming work.

The authors thank Alexander Tagantsev, Alexander Belov, and Vladimir Alshits for useful discussions and Uwe Jahn for a critical reading of this manuscript. K.K.S. acknowledges the support of the Russian Science Foundation under Grant No. 14-11-00083.

[1]S. J. Rosner, E. C. Carr, M. J. Ludowise, G. Girolami, and H. I. Erikson, Appl. Phys. Lett. **70**, 420 (1997).
[2]T. Sugahara, H. Sato, M. Hao, Y. Naoi, S. Kurai, S. T. K. Yamashita, K. Nishino, L. T. Romano, and S. Sakai, Jpn. J. Appl. Phys., Part 2 **37**, L398 (1998).
[3]J. S. Speck and S. J. Rosner, Physica B **273**, 24 (1999).
[4]N. Pauc, M. R. Phillips, V. Aimez, and D. Drouin, Appl. Phys. Lett. **89**, 161905 (2006).
[5]N. M. Shmidt, O. A. Soltanovich, A. S. Usikov, E. B. Yakimov, and E. E. Zavarin, J. Phys.: Condens. Matter **14**, 13285 (2002).
[6]D. Nakaji, V. Grillo, N. Yamamoto, and T. Mukai, J. Electron Microsc. **54**, 223 (2005).
[7]E. B. Yakimov, S. S. Borisov, and S. I. Zaitsev, Semiconductors **41**, 411 (2007).
[8]N. Ino and N. Yamamoto, Appl. Phys. Lett. **93**, 232103 (2008).
[9]E. B. Yakimov, Appl. Phys. Lett. **97**, 166101 (2010).
[10]E. B. Yakimov, J. Alloys Compd. **627**, 344 (2015).
[11]K. K. Sabelfeld, V. M. Kaganer, C. Pfüller, and O. Brandt, J. Phys. D: Appl. Phys. **50**, 405101 (2017).
[12]I. S. Smirnova, Sov. Phys.–Solid State **15**, 1543 (1974).
[13]C. Shi, P. M. Asbeck, and E. T. Yu, Appl. Phys. Lett. **74**, 573 (1999).
[14]E. H. Yoffe, Philos. Mag. **6**, 1147 (1961).
[15]J. Lothe, in *Elastic Strain Fields and Dislocation Mobility*, edited by V. L. Indenbom and J. Lothe (North-Holland, Amsterdam, 1992), Sect. 6.3, Chap. 5.
[16]V. Taupin, C. Fressengeas, P. Ventura, M. Lebyodkin, and V. Gornakov, J. Appl. Phys. **115**, 144902 (2014).
[17]J. F. Nye, *Physical Properties of Crystals* (Clarendon Press, Oxford, 1957).
[18]L. D. Landau and E. M. Lifshitz, *Electrodynamics of Continuous Media* (Pergamon Press, London, UK, 1960).
[19]B. A. Auld, *Acoustic Fields and Waves in Solids* (Wiley, New York, 1973), Chap. 8, Vol. I.

[20]J. P. Nowacki and V. I. Alshits, in *Dislocations in Solids*, edited by F. R. N. Nabarro and J. P. Hirth (Elsevier, Amsterdam, 2007), Chap. 72, Vol. 13, pp. 47–79.
[21]L. C. Lew Yan Voon and M. Willatzen, J. Appl. Phys. **109**, 031101 (2011).
[22]R. Maranganti and P. Sharma, Phys. Rev. B **80**, 054109 (2009).
[23]J. Hong and D. Vanderbilt, Phys. Rev. B **88**, 174107 (2013).
[24]P. V. Yudin and A. K. Tagantsev, Nanotechnology **24**, 432001 (2013).
[25]A. Y. Belov, in *Elastic Strain Fields and Dislocation Mobility*, edited by V. L. Indenbom and J. Lothe (North-Holland, Amsterdam, 1992), Sect. 2.5, Chap. 6.
[26]A. Polian, M. Grimsditch, and I. Grzegory, J. Appl. Phys. **79**, 3343 (1996).
[27]M. Feneberg and K. Thonke, J. Phys.: Condens. Matter **19**, 403201 (2007).
[28]M. Winkelnkemper, A. Schliwa, and D. Bimberg, Phys. Rev. B **74**, 155322 (2006).
[29]L. D. Landau and E. M. Lifshitz, *Quantum Mechanics* (Pergamon Press, Oxford, UK, 1977), Sect.77, Problem 1.
[30]T. Yamabe, A. Tachibana, and H. J. Silverstone, Phys. Rev. A **16**, 877 (1977).
[31]J. R. Banavar, D. D. Coon, and G. E. Derkits, Jr., Appl. Phys. Lett. **34**, 94 (1979).
[32]D. Drouin, A. R. Couture, D. Joly, X. Tastet, and V. Aimez, Scanning **29**, 92 (2007).
[33]L. Merten, Z. Naturforsch. A **21**, 793 (1966).
[34]G. Faivre and G. Saada, Phys. Status Solidi B **52**, 127 (1972).
[35]K. Shintani, J. Appl. Phys. **69**, 8119 (1991).